Analyst

Cite this: *Analyst*, 2011, **136**, 4500

www.rsc.org/analyst

PAPER

Three-dimensional network polyamidoamine dendrimer-Au nanocomposite for the construction of a mediator-free horseradish peroxidase biosensor

Jiao Luo,[ab] Mingnan Dong,[a] Fanbo Lin,[a] Meiling Liu,[a] Hao Tang,[a] Haitao Li,[a] Youyu Zhang*[a] and Shouzhuo Yao[a]

Received 22nd June 2011, Accepted 28th July 2011
DOI: 10.1039/c1an15515f

A three-dimensional network PAMAM-Au nanocomposite (3D-PAMAM-Au NC) was prepared by using the first generation polyamidoamine dendrimer (G1 PAMAM) as the dispersant agent. The resultant 3D-PAMAM-Au NC was successfully used as an immobilization matrix for the construction of a reagentless mediator-free horseradish peroxidase (HRP)-based H_2O_2 biosensor on a multi-walled carbon nanotubes (MWCNTs) modified glassy carbon electrode. With the advantages of the three-dimensional network, the organic–inorganic hybrid materials dramatically facilitate the direct electron transfer of HRP, and good bioelectrocatalytic activity towards H_2O_2 was demonstrated. Under optimum conditions, the current response of the enzyme modified electrode at −0.30 V was detected. The current response is linearly correlated to H_2O_2 concentration within the range of 18.00 μM to 20.80 mM with a correlation coefficient of 0.9992 and a sensitivity of 377.78 μA mM^{-1} cm^{-2}. The detection limit was down to 6.72 μM ($S/N = 3$). Furthermore, the biosensor exhibits some other excellent characteristics, such as high selectivity, short response time, and long-term stability. The 3D-PAMAM-Au NC has proved to be a promising biosensing platform for the construction of mediator-free biosensors, and may find wide potential applications in biosensors, biocatalysis, bioelectronics and biofuel cells.

1. Introduction

As an essential mediator, hydrogen peroxide (H_2O_2) is of great importance in industry, food, clinical control, and environmental protection.[1–3] Numerous techniques have been employed for the determination of H_2O_2, such as titrimetry,[4] chemiluminescene,[5] spectrometry,[6] and electrochemistry.[7–13] Horseradish peroxidase (HRP),[13] a heme enzyme, is generally used as a model system for the study of electron transfer in enzyme reaction systems and shows perfect catalysis activity to the reduction of H_2O_2 due to the interior electroactive iron hemes. However, the direct adsorption of HRP onto an electrode surface often results in denaturization and a consequent loss of the bioactivity. Moreover, HRP does not display electroactivity on bare electrodes due to the deep burying of electroactive groups within the protein structure.[14] Therefore, it is necessary to select a host matrix which can both provide a suitable microenvironment for proteins and also accelerate the direct electron transfer between proteins and the underlying electrode. Various materials have been employed for this purpose, such as nanoparticles,[15,16] conductive polymer films,[17] carbon nanotubes (CNTs),[18] DNA films,[19] ionic liquids,[20] mesoporous silicates[21] and so on. However, the lifetime and sensitivity of H_2O_2 biosensors still need to be improved in bioanalysis.

As a new type of macromolecule, dendrimers have been attracting increasing interest in many fields due to their excellent characteristics such as a regularly branched treelike structure, a high density of surface active groups, good structural homogeneity, high internal porosity and so on.[22–24] Poly(amidoamine) (PAMAM) has a three-dimensional structure and good biocompatibility. With high generation numbers ($G \geq 4$), PAMAM possesses a nearly spherical shape[25] and is usually applied in the construction of organic or hybrid nanostructure films or as templates for the synthesis of nanoparticle complexes.[26] In aqueous solution, PAMAM with terminal amino groups has different surface charges at different pH[27] and can be used to construct layer-by-layer assembly films with other species by electrostatic interactions.[28,29] For instance, Shi and co-workers developed a pesticide biosensor prepared by layer-by-layer assembly of acetylcholinesterase (AChE) and PAMAM-Au on a CNTs modified electrode.[29] In Hu's work,[30] G4-PAMAM was used to assemble multi-layer $\{PAMAM/protein\}_n$ films containing heme proteins and heme proteins' direct electrochemistry was realized. However, a novel material with

[a]*Key Laboratory of Chemical Biology & Traditional Chinese Medicine Research (Ministry of Education, China), College of Chemistry and Chemical Engineering, Hunan Normal University, Changsha, 410081, P R China. E-mail: zhangyy@hunnu.edu.cn; Fax: +86 731-88872046; Tel: +86 731-88872046*
[b]*ChangSha Environment Protection Agency, Changsha, 410081, P R China*

three-dimensional network structure, high specific surface area, and high loading capacity for enzyme, good catalytic properties, and perfect conductivity for electrons, is still required for the development of a highly sensitive and selective biosensor.

In this work, a novel three-dimensional network PAMAM-Au nanocomposite (3D-PAMAM-Au NC) was first prepared and utilized as a host matrix for constructing an HRP biosensor (see Fig. 1). The stable 3D-PAMAM-Au NC in aqueous medium was synthesized by the chemical reduction of $HAuCl_4$ in the presence of G1-PAMAM. In the preparation of 3D-PAMAM-Au NC, G1-PAMAM acted as a stabilization reagent or template due to its plentiful surface functional groups. On the one hand, Au nanoparticles could act as a good electronic conductor to promote the electron transfer of electroactive proteins and the three-dimensional network PAMAM-Au nanocomposite could serve as a biocompatible material and provide a suitable microenvironment for retaining the HRP activity. The electrostatic interaction of oppositely charged species was utilized to enhance the stability of the enzyme modified electrode. As compared to other biosensors, the 3D-PAMAM-Au NC is a promising biosensing platform for the construction of mediator-free biosensors with higher sensitivity and a fast response for the determination of H_2O_2.

2. Experiments

2.1 Instruments and chemicals

A Varian-500 high resolution NMR spectrometer (Bruker AVANCE DRX500, Switzerland) and a Thermo-Finnigan LCQ-Advantage mass spectrometer (GCMS-QP2010, Japan) were used to confirm the structure of the compounds. All absorbance measurements were carried out on a UV-2450 spectrophotometer equipped with 1.0 mL quartz cells (Shimadzu, Japan). The FTIR spectra were obtained with a Nicolet 670 IR spectrophotometer (Nicolet, USA). The morphology and particle size distribution were characterized using a transmission electron microscope at 100 kV (TEM, JOEL-1230, Japan).

$PAMAM\text{-}NH_2$ (G1) was synthesized according to ref. 31 and characterized by NMR, mass spectrometry and FT-IR spectroscopy. ^{1}HNMR ($CDCl_3$, 500 MHz): δ2.47 (4H, s), δ2.70 (8H, t), δ2.36 (8H, t), δ3.26 (8H, t), δ2.78 (8H, s), δ1.96 (8H, s). ^{13}C NMR ($CDCl_3$, 500 MHz): δ50.8 (2C), 49.7 (4C), 33.4 (4C), 41.7 (4C), 40.8 (4C), 172.2 (4NC═O). *m/z* (%): 517 (100). IR (KBr): 2950, 2900 (–CH_2–), 3250, 3050 (–NH–), 1650, 1550 (–NH–CO–) cm^{-1}. Horseradish peroxidase (HRP, EC 1.11.1.7, 300 U mg^{-1}) was purchased from Shanghai Jiehui Engineering Co., Ltd. and was used without further purification. MWCNTs (multi-walled carbon nanotubes; diameter: 20–40 nm, length: ~20 μm) were purchased from Chengdu Organic Chemical Co. Ltd., Chinese Academy of Science. All other chemicals were of analytical grade. Double-distilled water and freshly prepared solutions were used throughout the experiments.

2.2 Synthesis of PAMAM-Au nanocomposite

PAMAM-Au nanocomposite was prepared as follows:[32] 10 mL $HAuCl_4$ (0.5 mM) was added to 10 mL PAMAM (0.25 mM) solution and vigorously stirred for 1 h at room temperature. Then, 0.5 mL of $NaBH_4$ (0.01 M) was added dropwise into the solution. When gold nanocomposite was formed, the color changed from pale yellow to reddish brown. The pure gold nanoparticles were synthesized for comparison.[33]

2.3 Preparation of the HRP-PAMAM-Au/CNT/GCE modified electrode

A 3 mm diameter glassy carbon electrode (GCE) was polished to a mirror-like surface with 0.1 and 0.03 μm alumina slurries

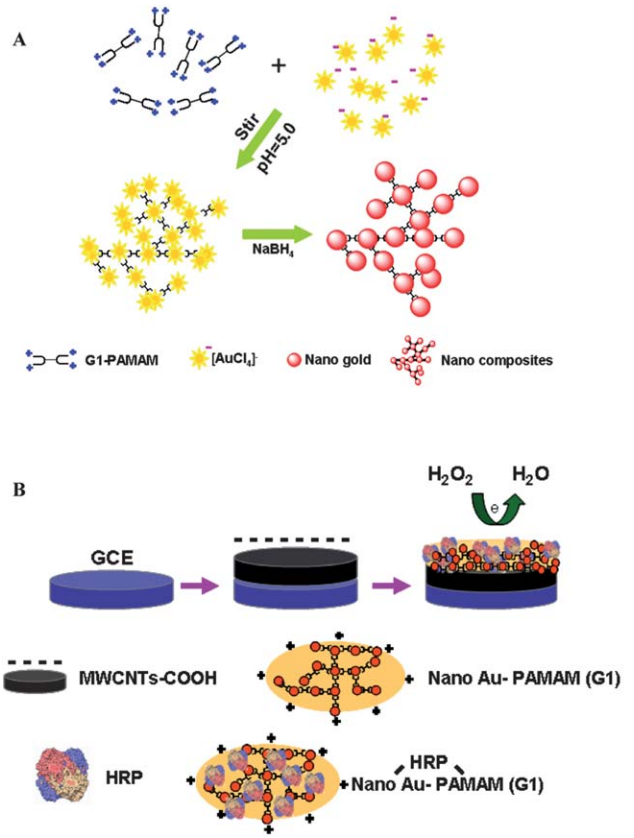

Fig. 1 (A) Illustration for the synthesis process of PAMAM-Au nanocomposite and (B) the preparation of the enzyme modified electrode.

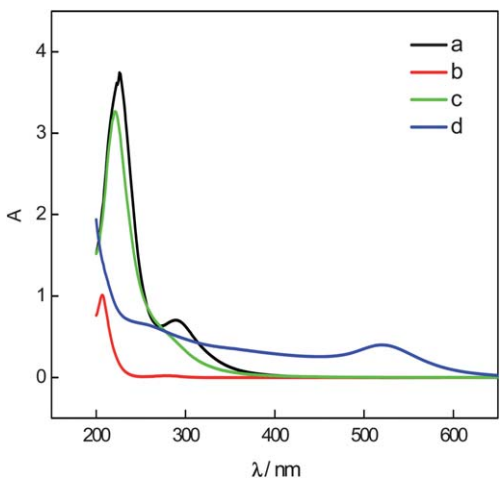

Fig. 2 UV-vis absorption spectra of (a) 0.25 mM $HAuCl_4$; (b) 0.25 mM $PAMAM\text{-}NH_2$; (c) the mixture of $HAuCl_4$ and PAMAM after stirring for 1 h; (d) PAMAM-Au nanocomposite.

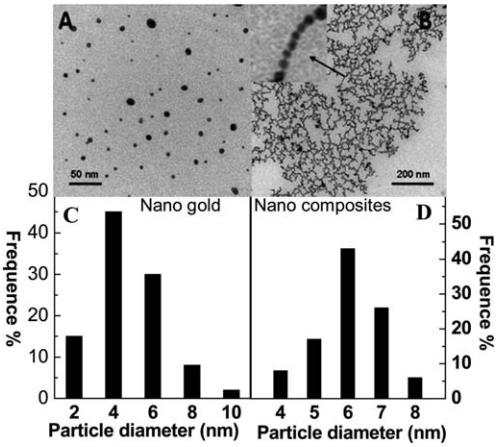

Fig. 3 TEM images and particle size distribution diagrams of pure nano gold (A, C) and 3D-PAMAM-Au NCs (B, D).

and washed with double-distilled water. The electrode was then pretreated electrochemically in 0.2 M $HClO_4$ aqueous solution by potential cycling within the potential range of 0 to 1.6 V at a scan rate of 50 mV s^{-1} until a stable cyclic voltammogram was obtained. 4 μL of acid-treated MWCNT suspension (10 mg mL^{-1}) was dropped onto the surface of the pretreated GC electrode and dried under an infrared lamp to form the CNT modified electrode. 10 μL of HRP-PAMAM-Au nanocomplex was dropped onto the MWCNT modified electrode and dried in a refrigerator at 4 °C and then the enzyme-modified electrode was obtained. The HRP-PAMAM-Au nanocomplex was obtained as follows: 500 μL of PAMAM-Au nanocomplex solution was mixed with different volumes of HRP solution (1 mg mL^{-1}, dispersed in 0.05 M PBS, pH 6.90). The mixture was stored in a refrigerator at 4 °C overnight. Excess HRP was removed by centrifugation. Then the precipitates were washed with 0.05 M PBS and redispersed in double-distilled water (pH 5.0). The enzyme-modified electrode was stored in a refrigerator at 4 °C.

2.4 Electrochemical determination

Electrochemical measurements were performed on a CHI 660C electrochemical workstation with a conventional three-electrode cell. A GCE served as the working electrode. A Pt foil and a KCl-saturated calomel electrode (SCE) were used as the counter electrode and the reference electrode, respectively. All the potentials were reported with respect to the SCE. Except as specifically stated, the electrochemical experiments were carried out in a 0.05 M phosphate butter solution (PBS, with 0.2 M $NaSO_4$ as the supporting electrolyte, pH 6.90) at room temperature (25 °C ± 1). All electrochemical experiments were performed under a nitrogen atmosphere and the solution was

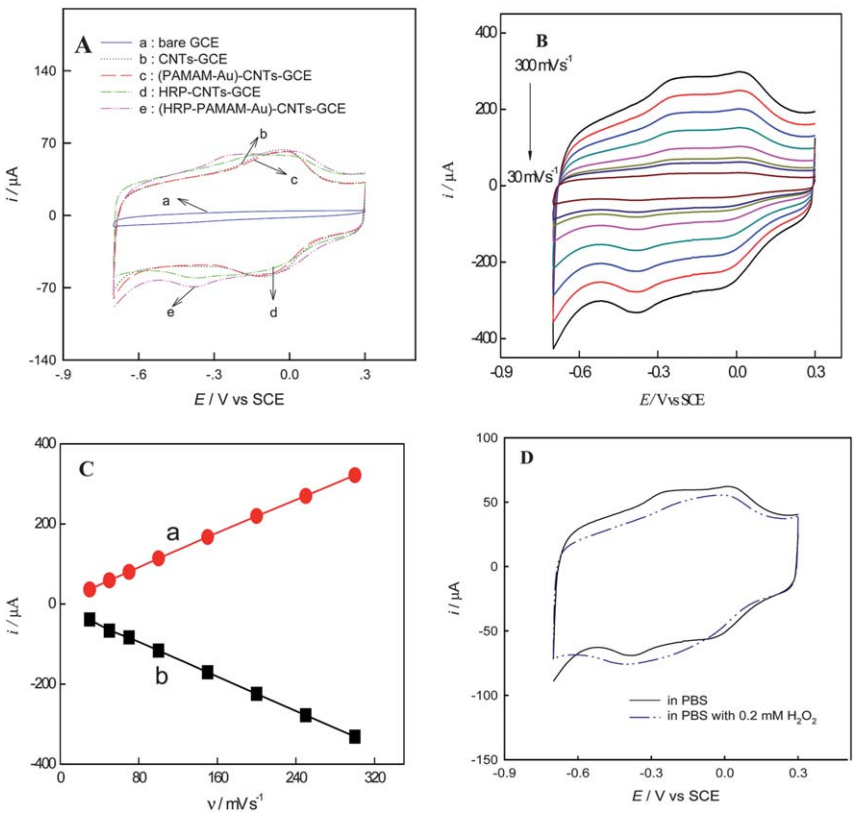

Fig. 4 (A) Cyclic voltammograms of different electrodes in 0.05 M deoxygenated PBS (pH 6.90) at a scan rate of 50 mV s^{-1}. (a) Bare GCE; (b) CNT/GCE; (c) (PAMAM-Au)/CNT/GCE; (d) HRP/CNT/GCE; and (e) (HRP-PAMAM-Au)/CNT/GCE. (B) Cyclic voltammograms of (HRP-PAMAM-Au)/CNT/GCE in 0.05 M pH 6.90 PBS at different rates. (C) The relationship of peak currents *vs.* scan rates. (D) Cyclic voltammograms of the (HRP-PAMAM-Au)/CNT/GC electrode in 0.05 mM PBS solution (pH = 6.90) with (dashed lines) and without (solid lines) 0.2 mM H_2O_2. Scan rate: 50 mV s^{-1}.

deoxygenated by bubbling with high-purity nitrogen prior to the experiments.

3. Results and discussion

3.1 Three-dimensional network PAMAM-Au nanocomposite

Fig. 2 shows the absorption spectra of the prepared 3D-PAMAM-Au NC. Curve a, b, c and d are the UV-vis absorption spectra of PAMAM, $HAuCl_4$, and the mixture of PAMAM-$HAuCl_4$ after stirring for 1 h and PAMAM-Au nanocomposite, respectively. As shown in Fig. 2, the PAMAM-$HAuCl_4$ has a ligand-to-metal charge-transfer band at 221 nm, at the same time the characteristic absorption peak of $[AuCl_4]^-$ at 289 nm[34] disappeared after stirring, which indicated the formation of a new complex.[35] After the addition of $NaBH_4$, a new absorption peak at 519 nm appeared which was attributable to the nanometre gold plasma resonance absorption. The appearance of the peak indicates the formation of gold nanoparticles in the system. The TEM image also confirms the formation of nanocomposites as shown in Fig. 3. The mean size of the nanocomposite particles is approximately 6.59 nm and is mainly within the 5–7 nm range (Fig. 3D). The nanocomposite exhibits a three-dimensional network structure (Fig. 3B). As a comparison, pure gold nanoparticles were also synthesized and characterized. The particle size of the pure gold nanoparticles is mainly within the range of 2–4 nm as shown in Fig. 3 A and C.

3.2 Direct electrochemistry of HRP immobilized in PAMAM-Au/CNT/GC electrode

Fig. 4A presents the cyclic voltammograms of the bare GC, CNT/GC, (PAMAM-Au)/CNT/GC, HRP/CNT/GC and (HRP-PAMAM-Au)/CNT/GC electrodes in a 0.05 M deoxygenated PBS (pH 6.90) at a scan rate of 50 mV s^{-1}. It can be seen that the background current of the CNT modified electrode is larger than that of the bare GC electrode, suggesting that the surface area of the CNT/GC must be greater than the effective area of the bare GC electrode. As shown in Fig. 4, a couple of redox peaks can be observed on all the modified electrodes containing carbon nanotubes. At a scan rate of 50 mV s^{-1}, the cathodic and anodic peak potentials are −0.109 and −0.004 V *vs.* SCE, respectively. This couple of peaks correspond to the redox of the carboxylic acid group.[36] As shown in Fig. 4A (curves d and e), after the immobilization of HRP, another pair of well-defined and nearly reversible peaks was observed, which indicated that the direct electron transfer between the HRP and modified electrode was realized. The anodic peak potential (E_{pa}) and cathodic peak potential (E_{pc}) are −0.24 V and −0.37 V (*vs.* SCE), respectively, which are close to the characteristic values of the Fe(III)/Fe(II) redox couple of the HRP heme prosthetic group reported previously.[10,11,14] Obviously, the peak current obtained from (HRP-PAMAM-Au)/CNT/GC electrodes was higher than that obtained from the HRP/CNT/GC electrode. The experiment results demonstrated that the three-dimensional network PAMAM-Au provided a biocompatible microenvironment for HRP. This direct electrochemical response of HRP should be attributed to the cooperative effect of HRP, PAMAM-Au, and CNT.

The effect of the scan rate on the cyclic voltammetric performance of (HRP-PAMAM-Au)/CNT/GCE was also investigated. Fig. 4B shows the CV curves of the enzyme electrode at various scan rates and the plot of the peak currents *vs.* scan rates. It can be seen that the redox peak currents increase with an increase in scan rate. As shown in Fig. 4C, the anodic (curve a) and cathodic

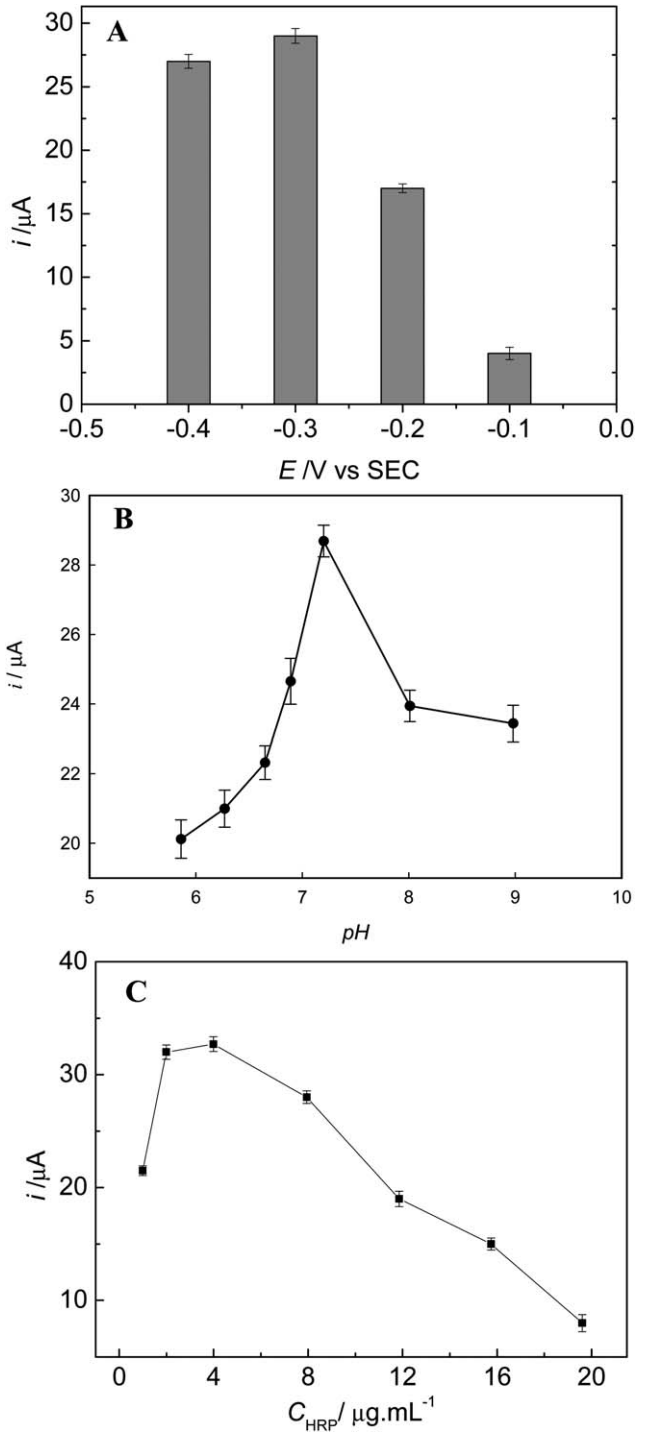

Fig. 5 The effect of applied potential (A), solution pH (B) and HRP volume (C) on the stable response current of (HRP-PAMAM-Au)/CNT/GC electrode in 0.05 mM PBS (pH 6.90). The error bars indicate the S.D. of three independent experiments. Hydrogen peroxide concentration: 0.2 mM. Scan rate: 50 mV s^{-1}.

(curve b) peak currents are found to be linearly related to the scan rate within the range of 30 mV s^{-1} to 300 mV s^{-1}, indicating that the tested cyclic voltammetric performance is a typical surface-controlled electrochemical process. It has been reported that heme-proteins, such as myoglobin, cytochrome c, and HRP, can catalyze the reduction reaction of H_2O_2. In order to check the catalytic activity of HRP in the (HRP-PAMAM-Au)/CNT/GCE, the electrocatalytic reduction of H_2O_2 was tested with cyclic voltammetry. With the addition of 0.20 mM H_2O_2 into pH 6.90 PBS, a significant increase in the cathodic peak at about −0.37 V and a decrease in the anodic peak current are observed as shown in Fig. 4D. This suggests that the immobilized HRP can catalyze the reduction of H_2O_2.

3.3 Optimization of experimental conditions

In order to optimize the experimental conditions, some factors such as applied potentials, pH, and enzyme content were investigated. The effect of applied potentials on the reduction of H_2O_2 was studied by chronoamperometry, as shown in Fig. 5A. It can be observed that the response current at the (HRP-PAMAM-Au)/CNT/GC electrode with an applied potential of −0.3 V is about 6.6 times than that at −0.1 V. When the potential was negatively shifted to −0.4 V, the response of the currents decreased a little and the noise increased observably. Therefore, a potential of −0.3 V was selected as the applied potential. The effect of pH on the enzyme electrode response was also investigated while varying the pH value from 5.86 to 8.98 in the presence of 1 mM H_2O_2 (Fig. 5B). The chronoamperometry results show that the maximum value of the current response at −0.3 V was obtained at pH 6.90. Thus, a buffer solution of pH 6.90 containing 0.05 M PBS was chosen throughout this work. The effect of HRP content in PAMAM-Au nanocomposites on the enzyme electrode response was studied by varying the HRP concentration in 500 μL PAMAM-Au nanocomplex solution (as shown in Fig. 5C). When the HRP concentration increased, the current response increased, and the maximum response was obtained at 4 μg mL^{-1} of the HRP solution. When the HRP concentration was increased further, there was almost no change in the response. Thus, 4 μg mL^{-1} HRP solutions were used to construct the enzyme electrode.

3.4 The electrocatalytic properties of (HRP-PAMAM-Au)/CNT/GCE toward the reduction of H_2O_2

In order to investigate the electrocatalytic properties of (HRP-PAMAM-Au)/CNT/GCE towards the reduction of H_2O_2, the current–time response curve of the electrode under the optimum conditions were recorded while continuously adding H_2O_2 solution to the test solution and the results are shown in Fig. 6. The steady state current was linear relative to the H_2O_2 concentration within the range of 18 μM to 20.80 mM. The linear regression equation was $i/\mu A = 26.8c + 2.3$, with a correlation coefficient of 0.999 ($n = 20$), where i refers to the steady state current and c refers to the H_2O_2 concentration. The detection limit and sensitivity of the biosensor were estimated to be 6.72 μM ($S/N = 3$) and 377.78 μA mM^{-1} cm^{-2}, respectively. A steady state current of 95% of the maximum was achieved at about 3 s. Compared with other methods, the sensitivity is higher,[10,20,37] the response is faster[11,17] and the upper limit of detection is higher.[17,20,37] The results mentioned above demonstrate that the HRP immobilized on (HRP-PAMAM-Au)/CNT/GCE exhibited good catalytic ability and fast response for H_2O_2.

3.5 Stability and reproducibility of the biosensor

The stability of the (HRP-PAMAM-Au)/CNT/GCE was evaluated by examining the cyclic voltammetric peak currents of HRP after continuously scanning for 100 cycles over the potential range of −0.7 to 0.3 V at a scan rate of 50 mV s^{-1} in 0.05 M PBS (pH 6.90). Fig. 7A shows the normalized current response at −0.37 V. Obviously, the current response at −0.37 V remained almost unchanged, indicating that the enzyme modified electrode was stable in the buffer solution (represented in Fig. 7A). After the enzyme modified electrode was stored in 0.05 M PBS (pH 6.90) at 4 °C for 1 week, and 4 weeks, the peak current of the modified electrode retained 96% and 82% of its initial value, respectively. As shown in Fig. 7B, 5 modified electrodes were fabricated using a similar method to investigate the reproducibility of the biosensor. The normalized current responses of 5 modified membrane-electrodes for the

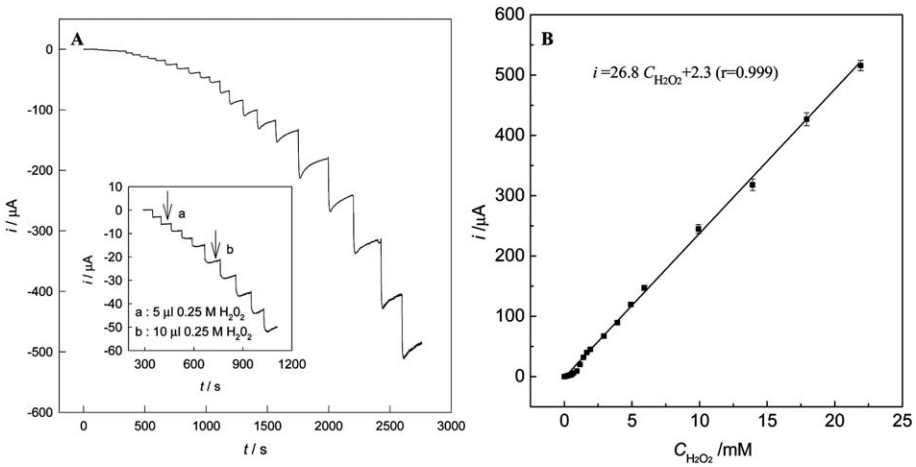

Fig. 6 (A) Current–time responses for successive addition of 5 mL of 250 mM H_2O_2 (a) or 10 μL of 250 mM H_2O_2 (b) at the (HRP-PAMAM-Au)/CNT/GC electrode recorded in 0.05 mM PBS (pH 6.90). (B) The current responses *vs.* H_2O_2 concentration. Potential applied: −0.3 V *vs.* SCE.

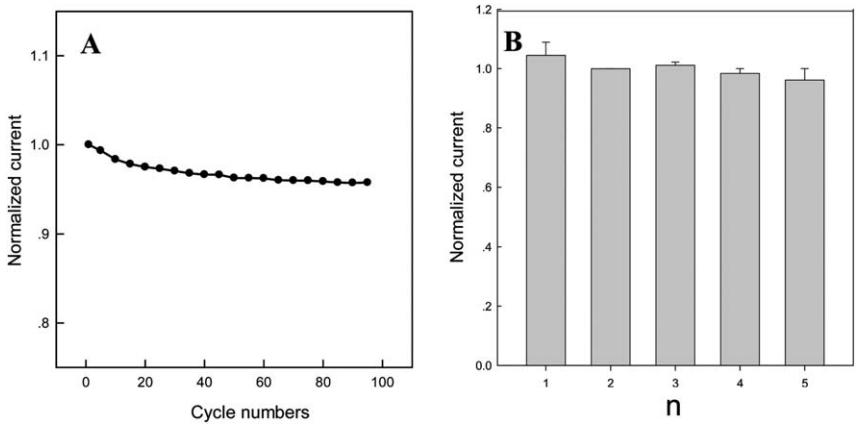

Fig. 7 (A) Normalized current response of the (HRP-PAMAM-Au)/CNT/GC electrode at −0.37 V during cyclic scanning for 100 cycles over the potential range of −0.7 to 0.3 V at a scan rate of 50 mV s^{-1} in 0.05 M PBS (pH 6.90). The current at −0.37 V for the first scan is defined as 1. (B) Normalized current response of five similar sensors for the determination of 1 mM H_2O_2 in 0.05 mM PBS solution (pH = 6.90). Mean current of five sensors is defined as 1. *n* refers to the electrode numbers.

determination of 1 mM H_2O_2 are almost equal. The relative standard deviation was 3.1%. This result suggested that the responses of the proposed biosensor are reproducible.

4. Conclusion

In summary, we demonstrated that 3D-PAMAM-Au NC can be synthesized by using the first generation polyamidoamine dendrimer (G1 PAMAM) as the dispersant agent. Specifically, we showed that 3D-PAMAM-Au NC can be successfully used as an immobilization matrix for the construction of a reagentless mediator-free horseradish peroxidase (HRP)-based H_2O_2 biosensor on a multi-walled carbon nanotubes (MWCNT) modified glassy carbon electrode. The unique capability of this biosensor is due to the advantages of the three-dimensional network of the organic–inorganic hybrid materials which dramatically facilitate the direct electron transfer of HRP resulting in good bioelectrocatalytic activity towards H_2O_2. The sensor displays a high sensitivity (377.78 μA mM^{-1} cm^{-2} and a linear response within a concentration range up to 20.80 mM for H_2O_2 determination. Furthermore, the biosensor exhibits some other excellent characteristics, such as high sensitivity and selectivity, short response time, and long-term stability. 3D-PAMAM-Au NC has been proved to be a promising biosensing platform for the construction of mediator-free biosensors, and may find wide potential applications in biosensors, biocatalysis, bioelectronics and biofuel cells.

Acknowledgements

This work was supported by the National Natural Science Foundation of China (20975037, 20705008, 21005037), and Scientific Research Fund of Hunan Provincial Science and Technology Departments (09JJ3019, 07JJ3024).

References

1 J. Kulys, L. Gorton, E. Domínguez, J. Emnéus and H. Jarskog, *J. Electroanal. Chem.*, 1994, **372**, 49–55.
2 E. S. Forzani, G. A. Rivas and V. M. Solis, *J. Electroanal. Chem.*, 1995, **382**, 33–40.
3 P. N. Bartlett, P. R. Birkin, J. H. Wang, F. Palmisano and G. De Benedetto, *Anal. Chem.*, 1998, **70**, 3685–3694.
4 E. C. Hurdis and H. Romeyn, *Anal. Chem.*, 1954, **26**, 320–325.
5 S. Hanaoka, J. M. Lin and M. Yamada, *Anal. Chim. Acta*, 2001, **426**, 57–64.
6 C. Matsubara, N. Kawamoto and K. Takamura, *Analyst*, 1992, **117**, 1781–1784.
7 M. Vreeke, R. Maidan and A. Heller, *Anal. Chem.*, 1992, **64**, 3084–3090.
8 M. G. Garguilo, H. Nhan, A. Proctor and A. C. Michael, *Anal. Chem.*, 1993, **65**, 523–528.
9 F. Gao, R. Yuan, Y. Chai, S. Chen, S. Cao and M. Tang, *J. Biochem. Biophys. Methods*, 2007, **70**, 407–413.
10 X. Chen, C. Fu, Y. Wang, W. Yang and D. G. Evans, *Biosens. Bioelectron.*, 2008, **24**, 356–361.
11 B. Wang, J. J. Zhang, Z. Y. Pan, X. Q. Tao and H. S. Wang, *Biosens. Bioelectron.*, 2009, **24**, 1141–1145.
12 Y. Zhang, Z. Tang, J. Wang, H. Wu, A. Maham and Y. Lin, *Anal. Chem.*, 2010, **82**, 6440–6446.
13 J. Zhao, Y. Zhang, H. Li, Y. Wen, X. Fan, F. Lin, L. Tan and S. Yao, *Biosens. Bioelectron.*, 2011, **26**, 2297–2303.
14 L. Zhang, Q. Zhang, X. Lu and J. Li, *Biosens. Bioelectron.*, 2007, **23**, 102–106.
15 J. Jia, B. Wang, A. Wu, G. Cheng, Z. Li and S. Dong, *Anal. Chem.*, 2002, **74**, 2217–2223.
16 Y. Xiao, H. X. Ju and H. Y. Chen, *Anal. Biochem.*, 2000, **278**, 22–28.
17 Y. T. Kong, M. Boopathi and Y. B. Shim, *Biosens. Bioelectron.*, 2003, **19**, 227–232.
18 L. Qian and X. Yang, *Talanta*, 2006, **68**, 721–727.
19 S. Xu, L. Li, Z. Du, L. Tang, Y. Wang, T. Wang and J. Li, *Electrochem. Commun.*, 2009, **11**, 327–330.
20 R. Yan, F. Zhao, J. Li, F. Xiao, S. Fan and B. Zeng, *Electrochim. Acta*, 2007, **52**, 7425–7431.
21 S. Wu, H. X. Ju and Y. Liu, *Adv. Funct. Mater.*, 2007, **17**, 585–592.
22 D. C. Tully and J. M. J. Frechet, *Chem. Commun.*, 2001, 1229–1239.
23 A. E. Beezer, A. S. H. King, I. K. Martin, J. C. Mitchel, L. J. Twyman and C. F. Wain, *Tetrahedron*, 2003, **59**, 3873–3880.
24 E. Emmrich, S. Franzka, G. Schmid and J. P. Majoral, *Nano Lett.*, 2002, **2**, 1239–1242.
25 K. Esumi, K. Miyamoto and T. Yoshimura, *J. Colloid Interface Sci.*, 2002, **254**, 402–405.
26 H. C. Yoon and H. S. Kim, *Anal. Chem.*, 2000, **72**, 922–926.
27 W. Chen, D. A. Tomalia and J. L. Thomas, *Macromolecules*, 2000, **33**, 9169–9172.
28 N. Krasteva, I. Besnard, B. Guse, R. E. Bauer, K. Müllen, A. Yasuda and T. Vossmeyer, *Nano Lett.*, 2002, **2**, 551–555.
29 Y. Qu, Q. Sun, F. Xiao, G. Shi and L. Jin, *Bioelectrochemistry*, 2010, **77**, 139–144.

30 L. Shen and N. Hu, *Biomacromolecules*, 2005, **6**, 1475–1483.
31 D. A. Tomalia, H. Baker, J. Dewald, M. Hall, G. Kallos, S. Martin, J. Roeck, J. Ryder and P. Smith, *Polym. J.*, 1985, **17**, 117–132.
32 B. F. Pan, F. Gao and H. C. Gu, *Polymer Materials Science & Engineering*, 2005, **21**, 224–227.
33 C. H. Kuo, T. F. Chiang, L. J. Chen and M. H. Huang, *Langmuir*, 2004, **20**, 7820–7824.
34 J. Wang, G. Liu, M. Rasul Jan and Q. Zhu, *Electrochem. Commun.*, 2003, **5**, 1000–1004.
35 D. Li and J. Li, *Chem. Phys. Lett.*, 2003, **372**, 668–673.
36 Z. H. Wang, J. Liu, L. S. Yan, Y. M. Wang and G. A. Luo, *Chinese.J. Anal. Chem.*, 2002, **30**, 1053–1057.
37 D. H. Fan, J. Y. Sun and K. J. Huang, *Colloids Surf., B*, 2010, **76**, 44–49.

